Journal of Pharmacokinetics and Pharmacodynamics, Vol. 31, No. 6, December 2004 (© 2005)
DOI: 10.1007/s10928-005-5912-0

Population Pharmacokinetic Modeling of Subcutaneously Administered Etanercept in Patients with Psoriasis

Ivan Nestorov,[1,*] Ralph Zitnik,[2] and Thomas Ludden[3]

The objective of this paper is to present a population PK model which adequately describes the time–concentration profiles of different doses of etanercept (Enbrel®) administered subcutaneously to subjects with moderate-to-severe psoriasis and to simulate the time courses of concentrations following 50 mg once weekly (QW) dosing. Pharmacokinetic (PK) data from three clinical studies with doses 25 mg QW, 25 mg twice weekly (BIW) and 50 mg BIW, were used. A one-compartment model with gender, weight and time covariates on the apparent clearance and weight covariate on the apparent volume of distribution was developed. The population mean of the apparent steady state clearance in males was 0.129 l/h, compared to 0.148 l/h in females. The clearance varied with time being lower in the first 2 weeks of the therapy, increasing sharply during weeks 3–4, and converging gradually after that to its steady state level. The population mean of the apparent volume of distribution also varied with time and was 16.1 l during week 1, 20.0 l during weeks 2–4 and 22.5 l after week 4. The population PK model adequately described the observed concentration–time profiles in subjects with psoriasis. Despite a somewhat different covariate set, the parameter estimates of the population PK model for etanercept are very similar between the psoriasis and rheumatoid arthritis populations. The population PK model was used to simulate the pharmacokinetic profiles after a novel 50 mg QW dosing regimen. The simulations show good agreement with the observed data from 84 subjects participating in a fourth study (50 mg QW dose) used as an external validation set. The simulations of the 50 mg QW and the 25 mg BIW dosing regimens show that there is a significant overlap between the profiles yielding similar steady state exposures with both dosing regimens. The latter is an indication that the respective efficacy and safety profiles after those two dosing regimens are likely to be similar.

KEY WORDS: etanercept; psoriasis; population pharmacokinetic model; simulation.

[1]ZymoGenetics, 1201 Eastlake Avenue East, Seattle, WA 98102, USA.
[2]Amgen Inc., One Amgen Center Drive, M.S. 30E-0-B, Thousand Oaks, CA 91320-1799, USA.
[3]GloboMax ICON, 7250 Parkway Drive, Suite 430, Hanover, MD 21076.
*To whom correspondence should be addressed. E-mail: intv@zgi.com

1567-567X/04/1200–0463/0

GLOSSARY:

ACR20	American College of Rheumatology response criteria of 20% improvement
AUC	area under the concentration curve
BIW	twice weekly
BMI	body mass index
BSA	body surface area formula = 0.007184* (weight in kg)$^{0.425}$* (height in cm)$^{0.725}$
BQL	below quantification limit
CI	confidence interval
CL	clearance
CL/F	apparent clearance
CRF	case report form
CSR	clinical study report
CV	coefficient of variation
C_{max}	maximum concentration
C_{min}	minimum concentration
df	degrees of freedom
DOPD	duration of psoriasis disease
ELISA	enzyme-linked immunosorbent assay
F	bioavailability
FDA	food and Drug Administration
FO	first-order
FOCE	first-order conditional estimation
GAM	generalized additive model analysis
IV	intravenous
IIV	interindividual variability
IOV	interoccasion variability
IV	intravenous
K_a	absorption rate constant
LLOQ	lower limit of quantification
n	number of subjects
nc	not calculated
NCA	noncompartmental analysis
ND	no data
NSAIDs	nonsteroidal anti-inflammatory drugs
OFV	objective function value
OCC	occasion
PASB	PASI score at baseline
PASI	psoriasis area and severity index
PD	pharmacodynamic(s)
PK	pharmacokinetic(s)
PSPT	prior systemic or phototherapy
QOL	quality of life
QW	once weekly
RA	rheumatoid arthritis
SC	subcutaneous
SD	standard deviation
TAD	time since last administered dose
TNF	tumor necrosis factor, cachectin (previously known as TNFα)
TNFR	tumor necrosis factor receptor
V	volume of distribution
V/F	apparent volume of distribution
WTKG	weight in kilograms

INTRODUCTION

Psoriasis is a chronic inflammatory disorder that affects approximately 2% of the world's population (1). Although psoriasis is rarely fatal, the impact of the disease on patients' lives is substantial, and has been consistently underestimated. Psoriasis disease is characterized by infiltration of the skin with activated T cells and by abnormal keratinocyte proliferation. Dysregulation of T cell antigen-presenting cell interactions and over-expression of proinflammatory cytokines play a central role in the pathogenesis of psoriatic skin lesions (2). As a result of over production by T cells and keratinocytes, tumor necrosis factor (TNF) levels are increased in psoriatic lesions compared with levels in uninvolved skin in patients and in normal individuals. Serum and lesional TNF levels decrease after effective psoriasis therapy, correlating with clinical improvement in the disease (3).

Etanercept (Enbrel®) is a novel dimeric fusion protein consisting of the extracellular ligand-binding protein of the human 75 kDa (p75) tumor necrosis factor receptor (TNFR) linked to the Fc portion of the human IgG1. Etanercept competitively inhibits the interaction of TNF with cell-surface receptors, preventing TNF-mediated cellular responses and modulating the activity of other proinflammatory cytokines that are regulated by TNF.

The safety and efficacy of etanercept has been demonstrated in subjects with rheumatoid arthritis (4, 5). To most adult rheumatoid arthritis (RA) patients, etanercept is administered at a dose of 25 mg twice weekly (BIW) as a subcutaneous (SC) injection, 72–96 h apart. A novel 50 mg once weekly (QW) SC dosing regimen has been approved recently by the FDA for RA, juvenile RA, ankylosing spondylitis, and psoriatic arthritis.

The safety and efficacy of etanercept has been demonstrated in subjects with psoriatic arthritis (6), where etanercept also improved psoriatic skin lesions. This observation led to three clinical studies, evaluating the efficacy of three dosing regimens (25 mg QW, 25 mg BIW, and 50 mg BIW) of etanercept in the treatment of chronic plaque psoriasis. In all studies etanercept treatment led to rapid, significant, and dose-dependent improvement in disease severity (7) — an indication that exposure is a determinant of the observed etanercept efficacy.

The majority of the available information on the pharmacokinetics (PK) of etanercept originates from studies with either healthy volunteers or RA subjects. The PK of the drug in psoriatic patients has not been characterized so far.

The PK of subcutaneously administered etanercept in healthy volunteers was best described by a one-compartment model using a two-stage approach (8). Etanercept is slowly absorbed from the site of injection with an absorption rate ($\pm$SD) of 0.0396 ± 0.025 h^{-1}. After a single subcutaneous administration of 25 mg dose the mean peak concentration is 1.46 ± 0.72 mg/l, achieved at a mean time of 51 ± 14 h. The elimination of etanercept in healthy subjects has a mean half-life of 68 ± 19 h, the apparent mean serum clearance (CL/*F*) is 0.132 ± 0.085 l/h. The AUC(0-∞) is 235 ± 98 mg h/l and the apparent volume of distribution (V/*F*) is 12 ± 6 l. Etanercept is well absorbed after SC injection, and the absolute bioavailability, estimated after single IV and SC doses in 6 healthy subjects, is approximately 58% (9).

After a single 25 mg SC injection of etanercept to RA subjects, the mean $\pm$ SD elimination half-life was 102 ± 30 h, the mean maximum concentration was 1.1 ± 0.6 mg/l, observed at a mean time of 69 ± 34 h, and the estimated apparent clearance was 0.16 ± 0.08 l/h (Enbrel® package insert). After 6 months of twice-weekly 25 mg dosing, the mean maximum concentration increased to 2.4 ± 1.0 mg/l.

An extensive nonlinear mixed effect modeling analysis has been performed to estimate the population PK/PD parameters of etanercept and their variability in RA patients (10). Cumulative area under the concentration–time curve (AUC) was used as an exposure variable, and the American College of Rheumatology response criteria of 20% improvement (ACR20) was the binomial clinical PD endpoint.

The overall objective of this paper is to present a population PK model which adequately describes and predicts the time–concentration profiles of different doses of etanercept administered to subjects with moderate-to-severe psoriasis and to explore the time courses of concentrations of 50 mg once weekly dosing of etanercept by simulation with the model developed. In order to achieve this objective, we had to achieve the following:

- Develop a population PK model which adequately describes and predicts the concentration–time profiles of different doses of etanercept administered to subjects with moderate-to-severe psoriasis.
- Estimate the population PK parameters and their variability, including interindividual, interoccasion, and residual variability.
- Identify significant and meaningful covariates which might influence population PK parameters and/or their variability.
- Explore the time courses of concentrations of 50 mg once weekly dosing of etanercept by simulation.

MATERIALS AND METHODS

Assumptions

The major general assumptions of our analysis were as follows:

- Concentration–time data sets from the three clinical studies in psoriasis, when pooled and analyzed together, will be an informative basis for explaining the population PK profiles of etanercept in this indication.
- Age, sex, race, body weight, height, body mass index (BMI), body surface area (BSA), treatment, duration of psoriatic disease (DOPD), psoriasis area and severity index (PASI) score at baseline (PASB), and prior systemic or phototherapy (PSPT) are candidate covariates for population PK parameters and/or their variability.

Other more specific assumptions made in the analysis are described elsewhere where pertinent.

Study Design

A summary of the study designs (11) is given in Table I. For all dosing arms response to etanercept therapy, based on a primary efficacy endpoint of a ≥75% improvement from baseline in the psoriasis area and severity index (PASI75) was rapid and sustained.

The demographic characteristics of the patients in the active treatment groups from all three studies are given in Table II.

Pharmacokinetic data from a new study (Study 4), initiated while the modeling program was in progress, were used as an external data set for additional validation of the population PK model. The design of this study is summarized in the last column of Table I. Etanercept was administered 50 mg QW by SC injection. Subjects who participated in Studies 2 or 3 were rolled over into Study 4.

Determination of Etanercept Concentrations in Serum

Serum concentrations of etanercept were measured by a validated enzyme-linked immunosorbent assay (ELISA) method. This ELISA method utilized a sandwich format to measure etanercept.

A mouse anti-TNFR:Fc monoclonal antibody was bound to the ELISA plate and used to capture etanercept in the standards, controls, or

Table I. Study Design Characteristics

	Model development dataset			External validation set
Design	Study 1	Study 2	Study 3 (7)	Study 4[a]
Type	Double blind, randomized Phase 2	Double blind, randomized Phase 3	Double blind, randomized Phase 3	Open label, Phase 3
Dose arms & mode of administration	Placebo, 25 mg BIW SC	Placebo,[b] 25 mg BIW, 50 mg BIW SC	Placebo,[b] 25 mg QWW, 25 mg BIW, 50 mg BIW SC	50 mg QW
Duration	24 weeks	12 weeks blinded period[c] Followed by up to 36 week open label 25 mg BIW SC	24 weeks blinded period[b] Followed by a withdrawal and re-treatment period (7)	4 weeks or more
PK sampling schedule	Before study start; weeks 12[d] and 24[d]	Before study start; weeks, 2,[d] 4,[d] 8,[d] and 12[d]	Before study start; weeks 2,[d] 4,[d] 8,[d] 12,[d] and 24[d] Intensive sampling ($n=41$): week 1, days 2, 3, 4, 7; week 12, days 77, 78, 80, 82; and week 24, days 161, 162, 164, 165, 167	After at least 4 weeks[e] of treatment: at 0, 24, 48, 96, 168 during the designated sampling week
ELISA characteristics	LLOQ 0.3 ng/ml Accuracy 1.3% to −24.9% Precision 9.8–13.8%	LLOQ 0.625 ng/ml Accuracy 13% to −13.6% Precision 6.5–14%	LLOQ 0.625 ng/ml Accuracy 6% to −21% Precision 9–14%	LLOQ 0.625 ng/ml Accuracy 13% to −13.6% Precision 6.5–14%

[a] $n=84$.
[b] Placebo patients started active treatment at week 12 of the studies.
[c] Only data from the blinded period included in the PK dataset.
[d] Trough samples by design.
[e] To emulate steady state.

Table II. Covariate Distribution of Subjects from Studies 1, 2, and 3

# Study	1[a]	2[a]	3[a]	Total[a]
# Subjects	55	635	387	1077
Sex, n (%)				
Male	33 (60.0%)	428 (67.4%)	257 (66.4%)	718 (66.7%)
Female	22 (40.0%)	207 (32.6%)	130 (33.6%)	359 (33.3%)
PSPT				
Yes	55 (100%)	484 (76.2%)	343 (88.6%)	882 (81.9%)
No	0 (0%)	151 (23.8%)	44 (11.4%)	195 (18.1%)
Race, n (%)				
Caucasian	49 (89.1%)	553 (87.1%)	351 (90.7%)	953 (88.5%)
Asian	0 (0%)	20 (3.2%)	13 (3.4%)	33 (3.1%)
Black	1 (1.8%)	22 (3.5%)	5 (1.3%)	28 (2.6%)
Hispanic	4 (7.3%)	35 (5.5%)	12 (3.1%)	51 (4.7%)
Indian	1 (1.8%)	0 (0%)	0 (0%)	1 (0.1%)
Native A	0 (0%)	1 (0.2%)	1 (0.3%)	2 (0.2%)
Other	0 (0%)	4 (0.6%)	5 (1.3%)	9 (0.8%)
Age (years)				
Median	50	45	45	45
(min, max)	(25–72)	(18–84)	(20–87)	(18–87)
Weight (kg)				
Median	91.0	92.0	85.0	89.0
(min, max)	(56.0–140)	(39.0–198)	(45.0–181)	(39.0–198)
Height (cm)				
Median	175	173	173	173
(min, max)	(152–193)	(126–208)	(138–196)	(126–208)
BMI (kg/m^2)				
Median	29.7	30.0	28.3	29.5
(min, max)	(21.1–47.5)	(11.6–62.1)	(17.2–55.8)	(11.6–62.1)
BSA (m^2)				
Median	2.03	2.07	2.00	2.03
(min, max)	(1.57–2.64)	(1.42–2.98)	(1.40–2.80)	(1.40–2.98)
Disease duration (years)				
Median	20.8	17.3	20.4	18.25
(min, max)	(3.08–48.9)	(0.250–59.3)	(0.830–64.6)	(0.25–64.6)
PASB				
Median	15.3	15.7	16.7	15.9
(min, max)	(6.00–39.9)	(5.70–55.8)	(4.00–57.3)	(4.00–57.3)

[a]For sex, race, numbers (%, column percent) are shown. For other variables, mean ± standard deviation, median, minimum & maximum values (in parenthesis) are displayed.

unknown samples. A polyclonal goat anti-TNFR:Fc antibody was added to complete the sandwich. A horseradish peroxidase-conjugated donkey anti-goat antibody was then used to detect the bound goat antibody. A TMB–H_2O_2 substrate for horseradish peroxidase was added to generate a colorimetric reaction to quantify etanercept. The reaction was stop-

ped with the addition of a stopping solution. The intensity of the color in each well is proportional to the quantity of etanercept in the assay system. The quantity of etanercept in an unknown sample was determined by calculating the response of the sample against the calibration curve regressed using a 4-parameter regression model.

The assays were conducted at Amgen Inc., Seattle, WA (Study 1), Covance Laboratories, Inc., Madison, WI (Studies 2 and 4) and MDS-Pharma, St. Laurent, Canada (Study 3). The ELISA characteristics are given in the last row of Table I.

Data Handling

The three data sets for the individual studies were checked for consistency with regard to the order of data items and a 10% quality control check was performed. They were then merged together to form 1 large data set. Time after dose (TAD) and occasion (OCC) were added as data items. Occasions were defined in such a way that they included different visits explicitly stated in the study protocol and/or different periods when clusters of concentration data were obtained, as shown in Table III. The finalized merged NONMEM dataset contained data from 1077 subjects with 32883 dosing records and 4291 concentration observation records.

Model Building Strategy

All analyses were carried out using NONMEM (version V). Both the first-order (FO) method and the first-order conditional estimation (FOCE) methods were used during the modeling process.

At the first step, different basic structural models without interoccasion variability were built and compared. Next for the population PK

Table III. Definition of Occasions

	Time range (h)	
OCC	Begin	End
1	0	504
2	505	1008
3	1009	1680
4	1681	2352
5	2353	3024
6	3025	3696
7	3697	4200

model interoccasion variability (IOV) was introduced. As the actual concentration sampling times varied around the nominal ones, the occasions were defined as shown in Table III.

In all cases, various covariance structures were explored and modeled by using OMEGA BLOCK in NONMEM. To guide this process, individual *post hoc* values of the parameters characterizing interindividual variability (IIV) were plotted against each other. Once a systematic correlation between two variability parameters was found, it was modeled and tested for significance.

After the basic structural model was determined, covariate effects on the PK parameters were sought graphically, and then tested through estimation. When preliminarily selecting meaningful covariates, the generalized additive model (GAM) analysis in Xpose was used (12, 13). For significant covariate(s) selected by the GAM analysis, a stepwise forward and backward approach was applied such that each covariate was added or deleted one at a time.

The log likelihood ratio test was the primary criterion used to determine the appropriateness of a covariate selection. Where possible, physiological relevance was considered in covariate selection. The categorical covariates considered were sex, race, treatment, and prior systemic or phototherapy (PSPT). These were generally modeled using indicator variables. The continuous covariates considered were age, weight, height, BMI, BSA, DOPD, and PASI score at baseline (PASB). These continuous covariates were first standardized to typical or data-derived median values (e.g. 90 kg for weight) and their effects were modeled as proportionally affecting parameters.

Finally, the models were refined by either reintroducing previously deleted covariate(s) or removing covariate(s) that already existed in it. In this model refinement process, more stringent cut-off values were applied when determining whether to include a certain covariate.

During the whole process of model development, graphical methods (utilizing S-plus, SigmaPlot or Excel software) were also employed to judge general goodness-of-fit. Plots of observed versus model-based population or individual *post hoc* predicted values and various residual plots were used to detect any significant systemic departure from the model fit.

Modeling Stochastic Variability

For the population PK analysis, the jth observation (etanercept plasma concentration) of the ith individual, Obs_{ij}, measured at time t_j was assumed defined by the following equation,

$$\mathrm{Obs}_{ij} = f(\theta_i, \mathrm{Dose}, t_j) + \varepsilon_{ij}$$

where f denotes the structural population model, θ_i is the vector of the PK parameters for the ith individual, and ε_{ij} represents the residual or unexplained intraindividual shift of the observation from the model prediction. It was assumed that ε_{ij} is symmetrically distributed around mean 0, with variance denoted by σ^2.

For θ_{ik}, the kth element of the ith individual's parameter vector, the following model was proposed:

$$\theta_{ik} = \theta_{\mathrm{pop},k} \cdot \exp(\eta_{ik}) \tag{2}$$

where $\theta_{\mathrm{pop},\,k}$ is the mean population parameter of the kth element and η_{ik} represents the shift of the parameter of the ith individual from the population mean. η_{ik} was further assumed to be independent multivariate normally distributed, with mean 0 and with a variance–covariance matrix Ω with diagonal elements $(\omega_1^2, \omega_2^2, \ldots, \omega_m^2)$ such that the $\omega_{\,k}$ is approximately the coefficient of variation of kth parameter with respect to the typical value, $\theta_{\mathrm{pop},k}$.

For residual error in the population PK analysis, additive, proportional, and combined additive and proportional random error models were tested.

Model Qualification

In order to estimate the confidence intervals (CI) of the model parameters of the population PK model, a bootstrap procedure was applied to construct re-sampled (with replacement) data sets from which new sets of parameters and their variability were estimated (16). There were 1000 bootstrapped re-samples, and a 95% CI for each parameter and variability was constructed taking the 2.5th and 97.5th percentiles of the resultant estimates.

The predictive performance of the population PK model was tested by simulation and comparison of the shape of the probability distribution of the simulated and experimental concentration–time profiles.

A further internal validation of the final model was performed by comparing the model predictions with the clinical data available for the existing dosing regimens. The model predictions were derived by simulating 10,000 subjects, grouped in 5 batches with each batch containing 20 trials with 100 subjects per trial. Each subject's concentration–time profile was calculated every 12 h for up to 4872 h. After the simulation, all simulated concentration–time profiles were pooled together and the 2.5,

25, 50, 75 and 97.5 percentiles for each time point were calculated and compared with the respective percentiles of the data.

As an external validation step, the pharmacokinetic profiles following the novel 50 mg QW dosing regimen were simulated using the final population PK model by simulating 10,000 subjects, as outlined in the previous section. All simulated concentration time profiles at steady state (week 24 in the simulation) were pooled together and the 2.5, 25, 50, 75 and 97.5 percentiles for each time point were calculated and compared with the data from a subset of subjects ($n = 84$) on the novel 50 mg QW dosing regimen in Study 4 (external validation data set).

RESULTS

Basic Structural Model Development

Figure 1 summarizes the important steps in the development of the basic structural PK model and the covariate search. Initially, a one-compartment model with first-order absorption and elimination and a simple diagonal form of the variance–covariance matrix was compared with a two-compartment model. The latter was not supported by the data.

At the next step, interindividual variability (IIV) was added to the parameters of the one-compartment model apparent clearance (CL/F), apparent volume of distribution (V/F), and absorption rate constant (K_a). Due to the limited information about the absorption in the data, NONMEM was only able to identify a diagonal form of the variance–covariance matrix, when IIV variability was attached to all three PK parameters. When a full variance–covariance matrix was specified, the covariance estimation became unstable. Finally a OMEGA BLOCK(2) matrix on CL/F and V/F and a separate diagonal OMEGA for K_a were estimated successfully. It was noted that the data did not support estimation of the IIV on both the V/F and the K_a of the one-compartment model. It was decided, consequently, to drop the estimation of an IIV term on the K_a while exploring more complex model structures.

At the next step, interoccasion variability was added with the occasions defined as shown in Table III. The addition of the interoccasion variability led to a significant decrease in the OFV.

During the preliminary processing and reporting of the PK data from the individual studies, an interesting pattern was identified. After an initial rise in the concentration–time profile during the first 2 weeks of doses, an unexpected drop in the profiles was observed, most evident around 4 weeks. After that, the accumulation resumed, leading, however, to somewhat lower steady state levels compared to what would have been

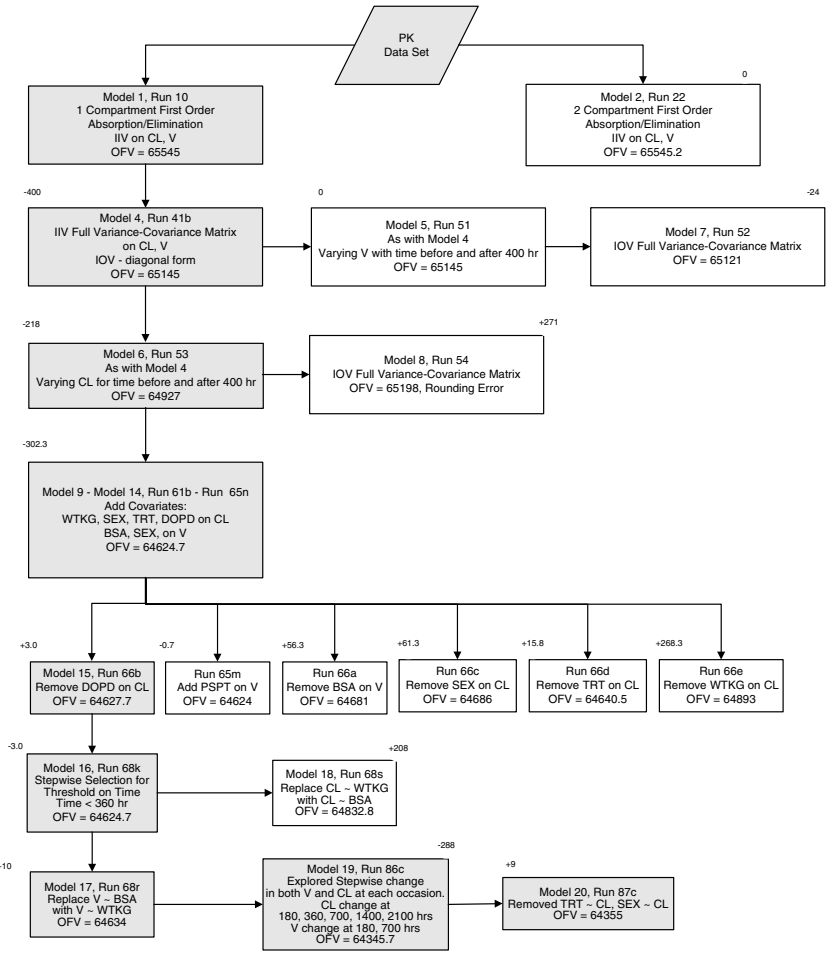

Fig. 1. Basic structural PK model selection (accepted models at each modeling step are shaded).

anticipated based on the first weeks profile. This phenomenon is illustrated in Fig. 2 (data from Study 3), where the mean trough profiles are shown. It was noted that the decrease in the concentrations between weeks 2 and 4 could be quite significant—around 30% of the average observed week 2 level. It was recognized that such a fluctuation could be caused by a one-off re-adjustment of the pharmacokinetic properties of the system after the first doses are administered.

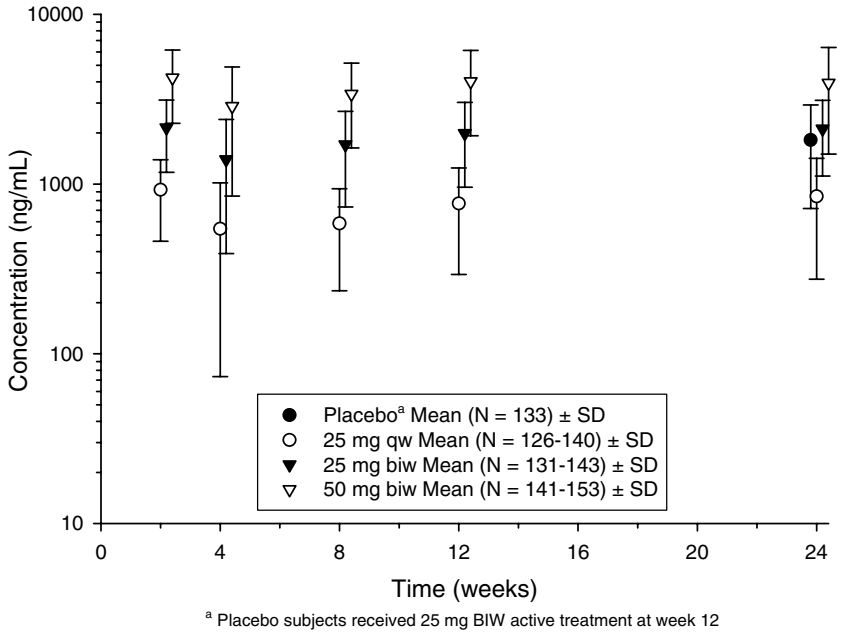

Fig. 2. Mean (±SD) etanercept serum concentration profiles for subjects in the active arms during weeks 0–24 of Study 3 (times slightly displaced for readability).

After several attempts to model a continuous (sigmoidal) time dependent change in the CL and V, which failed due to estimation convergence problems, this readjustment was modeled by introducing a binary covariate (TIME ≤ 400 h) on either CL/F or V/F. The stepwise change of clearance leads to a significant decrease in the objective function and was subsequently adopted in the model. Treated as a covariate, TIME has a somewhat unique connotation, implying a departure from the stationary (time-independent) pharmacokinetic models usually encountered.

Finally, a block form of the variance–covariance matrix was considered, which did not lead to significant decrease in the OFV but destabilized the estimation causing it to converge to local minima.

At various points during the basic model development unsuccessful attempts were made to return to a two-compartment structure.

The Basic Structural Model selected was the one-compartment first-order absorption and elimination (Model 6, Fig. 1) with IIV and IOV on CL/F and V/F, full variance covariance matrix of the IIV parameters,

diagonal form of the IOV variance covariance matrix and a binary covariate TIME ≤ 400 h on CL/F.

Covariate Selection

To facilitate the covariate identification process, a GAM fit was carried out using the individual Bayesian estimated CL/F and V/F from the basic structural model as dependent variables and the potential covariates as independent variables (12). The GAM procedure identified as significant covariates for CL/F: SEX, TRT, WTKG and DOPD, and for V/F: SEX, PSPT, HTCM and BSA.

Using this initial guidance, a thorough covariate search was carried out as shown in the lower panel of Fig. 1. Initially, the covariates, identified by GAM were added one by one and the likelihood ratio test was used to discriminate between rival models. The power terms on standardized body weight (on CL/F) and standardized BSA (on V/F) were also estimated. From the GAM identified covariates, inclusion of WTKG, DOPD, TRT and SEX on CL and BSA and SEX on V decreased the OFV significantly ($P < 0.05$)—Model 14, Fig. 1. In the model refinement process, the covariates that already existed in the model were removed one at a time, and the resultant objective function value was compared to the previous model.

At this point (Model 15), as the identified covariates BSA on V/F and WTKG on CL/F were strongly correlated, it was decided to convert the model to a unified covariate. Converting BSA to WTKG on V/F proved to increase the OFV by 9 points only, compared to 208 points increase when converting WTKG to BSA on CL/F. The former was adopted for the subsequent models.

Analyzing the goodness of fit plots during the covariate selection process, it was realized that the model with a single CL/F threshold at TIME ≤ 400 h is not flexible enough to accommodate adequately the fluctuation in the observed concentration–time profiles after the first weeks of dosing. An attempt to refine the single threshold resulted in a change from 400 to 360 h (Model 16) did not lead to a significant improvement. Consequently, after the identification of the major covariates, a full grid search with stepwise change in both CL/F and V/F at times 180, 360, 700, 1400, and 2100 h was carried out. Those grid nodes were selected as they separated the clusters of concentration measurements. The grid search resulted in the identification of 180, 360, 700, 1400, and 2100 h as significant thresholds for stepwise CL/F change and 180 h and 700 h as significant thresholds for V/F change (Model 19). It was noted that in the

latter run, the CL values between various treatments were very similar as were the V values for males and females.

Finally, TRT on CL/F and SEX on V/F were removed from the model, resulting in an increase in the OFV of 9 points (Model 20), which was not considered significant at the more rigorous ($P < 0.001$) level.

Population PK Model Finalization

After the completion of the covariate search using the FO method, several runs were made using the FOCE method with interaction option of NONMEM. The FOCE runs were unstable if IOV was included in the model, therefore efforts were focused on models without IOV without covariates or with covariate structures identified from the FO method. A large number of rounding errors occurred during estimation and the covariance step as a rule did not converge. The parameter estimates of the FOCE runs were similar to the corresponding FO runs (with IOV included). The diagnostic plots of the FOCE runs were inferior to the diagnostic plots of the respective FO runs (with IOV). Therefore, it was concluded that using a FOCE method with interaction (no IOV) was not sufficient to compensate for the abandonment of the IOV.

No improvement in the diagnostic plots was achieved during two runs with transformations (natural log and square root) of the data and the model.

It is well documented (10, 11, 15) that the baseline concentration samples for etanercept may sometimes be positive probably due to the presence of endogenous soluble TNF receptors in serum. Such positive baseline values are usually small and seldom exceed 1% of the maximum concentrations observed. For this reason it was decided not to model the baseline values and to delete all baseline samples from the final data set. The comparison of the results for the final population PK model structure with the initial data set, the data set with zero baseline concentrations removed and the data set with all baseline measurements removed shows that the parameter estimates are not sensitive to these input data manipulations.

Final Population PK Model

Based on the above results and considerations, the final form of the population PK model is one compartment first order linear model with apparent clearance and volume given by

$$\mathrm{Obs}_{ij} = \frac{F \cdot D}{V \cdot (k_a - k_{el})}\left(e^{-k_{el}t} - e^{-k_a t}\right) + \varepsilon_{ij} \tag{3}$$

where $k_{el} = \mathrm{CL}/V$ and

$$\mathrm{CL}/F\ (\mathrm{l/h}) = \left\{ \begin{array}{c} \text{Population Mean Males} \\ \text{Population Mean Females} \end{array} \right\} \times \text{TIME factor} \times (\mathrm{WTKG}/90)^{\text{Exponent on CL}} \tag{4}$$

$$V/F\ (\mathrm{L}) = \text{Population Mean} \times (\mathrm{WTKG}/90)^{\text{Exponent on V}} \tag{5}$$

The diagnostic plots of this model are shown in Fig. 3. There is a slight bias in the Individual Bayesian Predicted versus Observed Concentration plot, while the weighted residuals seem to be distributed symmetrically around the zero axis.

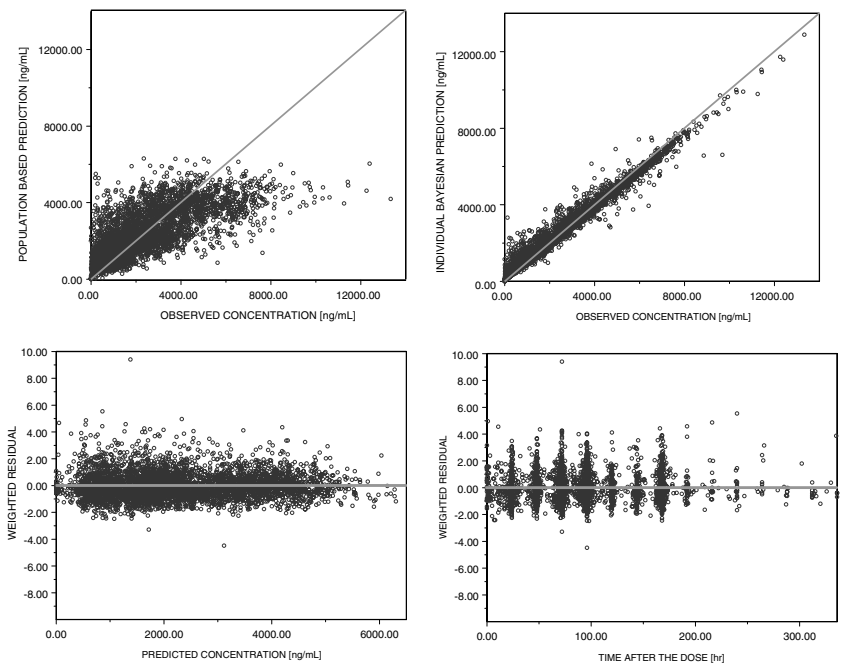

Fig. 3. Diagnostic plots for the final population PK model for etanercept in psoriasis. Clockwise from the upper left panel are observed values vs. population predicted values, observed values vs. individual bayesian predicted values, time after dose vs. weighted residuals, and predicted concentration values vs. weighted residuals.

The parameter estimates and the estimates of their IIV and IOV, together with the 95% confidence intervals (CI) derived from the bootstrap are given in Table IV. One hundred and forty three out of 1000 bootstrap runs, used to determine the confidence parameters of the model parameters resulted in NONMEM rounding error at three significant digits. The latter were rerun with four significant digits and only 70 of them resulted in NONMEM rounding error. As a result, the 95% confidence intervals for each parameter were calculated over 930 bootstrap runs.

It was noted that during bootstrap the resulting additive error term oscillated between insignificant levels (less than 2.5 ng/ml, i.e., less than 0.1–0.5% of the average concentration during active treatment) in 663 bootstrap runs, and a level of around 170 ng/ml (approximately 7–10% of average concentration during active treatment) in the rest. Both cases are shown in Table IV. The small value of the additive component, as well as the bootstrap results, show that the additive portion of the residual error could have been discarded from the model.

The population mean of the apparent clearance (CL/F, where F is the bioavailability) in males was 0.129 l/h (with a 95% CI of 0.123–0.136 l/h), compared to 0.148 l/h (95% CI of 0.137–0.161 l/h) in females. Interindividual variability of clearance was 32.7% (with a 95% CI of 30.0–35.7%) while interoccasion variability was 32.4% (95% CI of 25.7–36.2%). The clearance was lower in the first weeks of the therapy: 73.3% (95% CI of 52.3–93.5%) of the steady state value during week 1 (before 180 h), and 78.0% (95% CI of 67.0–89.2%) of the steady state value during week 2 (before 360 h). It increases sharply to 132% of the steady state value (95% CI of 124–141%) during weeks 3–4 (before 700 h), converging gradually after that to its steady state level. The clearance is related to the power 0.668 (95% CI of 0.551–0.829) of the median normalized subject body weight. The precision of the clearance and related estimates was high, possibly due to the large number of individuals in the data set.

The population mean of the apparent volume of distribution (V/F) was 16.1 l (95% CI of 10.1–20.7 l) during week 1 (before 180 h), 20.0 l (95% CI of 12.8–24.8 l) during weeks 2–4 (before 700 h) and 22.5 l (95% CI of 13.9–30.7 l) after week 4. The volume is related to the power 0.652 (95% CI of 0.0–0.973) of the median normalized subject body weight. Interindividual variability of volume was 20.9% (with a 95% CI of 8.9–43.6%) while interoccasion variability was 52.3% (95% CI of 35.1–92.9%). The precision of the volume and related estimates was still high, but lower than the precision in the clearance and related parameters.

The population mean of the first-order absorption rate constant (K_a) for etanercept was 0.0314 h^{-1} (95% CI of 0.0149–0.0533 h^{-1}). The precision of the K_a estimate is lower than the precision of the clearance and

Table IV. Parameter Estimates and Variability for Population PK Model of Etanercept in Psoriasis

Parameter	Symbol	Covariates	Population mean (95% C.I.¶)	Interindividual variability CV§ (95% C.I.¶)	Interoccasion variability CV§ (95% C.I.¶)
Clearance/F*	CL/F (l/h)	Male	0.129 (0.123~0.136)	32.7% (30.0~35.7%)	32.4% (25.7~36.2%)
		Female	0.148 (0.137~0.161)		
		Time ≤ 180 h˜	0.733 (0.523~0.935)		
		Time ≤ 360 h˜	0.780 (0.670~0.892)		
		Time ≤ 700 h˜	1.32 (1.24~1.41)		
		Time ≤ 1400 h˜	1.18 (1.11~1.26)		
		Time ≤ 2100 h˜	1.08 (1.03~1.13)		
		Time > 2100 h˜	1		
		Exponent on WTKG	0.668 (0.551~0.829)		
Volume of distribution/F*	V/F (l)	Time ≤ 180 h	16.1 (10.1~20.7)	20.9% (8.92~43.6%)	52.3% (35.1~92.9%)
		Time ≤ 700 h	20.0 (12.8~24.8)		
		Time > 700 h	22.5 (13.9~30.7)		
		Exponent on WTKG	0.652 (0~0.973)		
Absorption rate	K_a (hr^{-1})		0.0314 (0.0149~0.0533)		
Residual error#			Additive error (ng/ml)	Proportional error, CV§	
		$n = 663$	0 (0~0.000071)	24.3% (20.8~28.3%)	
		$n = 267$	174 (126~226)	21.7% (17.9~25.6%)	

*Calculated for a subject weighing 90 kg; F = bioavailability.
¶Confidence interval of estimate, calculated from 930 bootstrap re-samplings.
§Coefficient of variation.
#Calculated for 663 bootstrap re-samplings, see text.
˜TIME factor in Eq. (4).

volume due to the small number of data points in the absorption phase of the concentration–time profiles.

The inspection of the histograms of the random effect parameters characterizing the IIV (ETA(1) on CL/F and ETA(2) on V/F) and the parameters characterizing the IOV (ETA(3) through ETA(9) for OCC 1 through OCC 7 on CL/F and ETA(10) through ETA(16) for OCC 1 through OCC 7 on V/F) showed that virtually all ETA's are distributed symmetrically around zero.

Model Qualification—Internal Validation

Using the final population PK model and the covariate data for the adult psoriatic population, 10,000 subjects were simulated for each of the 2 dosing regimens—25 mg BIW and 50 mg BIW—over 30 weeks of dosing. The quartiles of the simulations were estimated and compared to the quartiles of the clinical data. The quartiles of the predictions generated from the final population PK model are generally within 10–20% of the quartiles calculated from the data. The good agreement between the predictions generated from the final population PK model and the experimental data is illustrated in Fig. 4 (25 mg BIW in upper panel and 50 mg BIW in lower panel), where the actual observed concentrations are overlaid upon the 2.5, 25, 50, 75 and 97.5 percentiles of the simulations, shaded with different intensity. A large proportion of the observed values falling below the shaded areas belong to individuals who have skipped doses or discontinued treatment, whereas the simulations were done with the nominal dosing scheme and could not have captured incompliance to the dosing scheme.

As seen from both panels, the final population PK model captures the central trend of the experimental data well, accounting for the observed fluctuation in the concentration levels between weeks 2 and 8. The final model also described well the existing variability in the data.

Simulations of the Novel 50 mg QW Dosage Regimen—External Validation

The 2.5, 25, 50, 75 and 97.5 percentiles obtained from the simulation of the novel 50 mg QW dosing regimen during steady state (week 24) are superimposed with the measured individual concentrations from study 4 as shown in Fig. 5. There is a good agreement between the predictions and the experimental data, both in terms of central tendency and in terms of the variability observed, with a slight under-prediction of the peak concentrations. One potential explanation is that by week 5 (the earliest time when the concentration sampling in Study 4 was scheduled to begin) some of the concentration–time profiles might not have converged to true steady state.

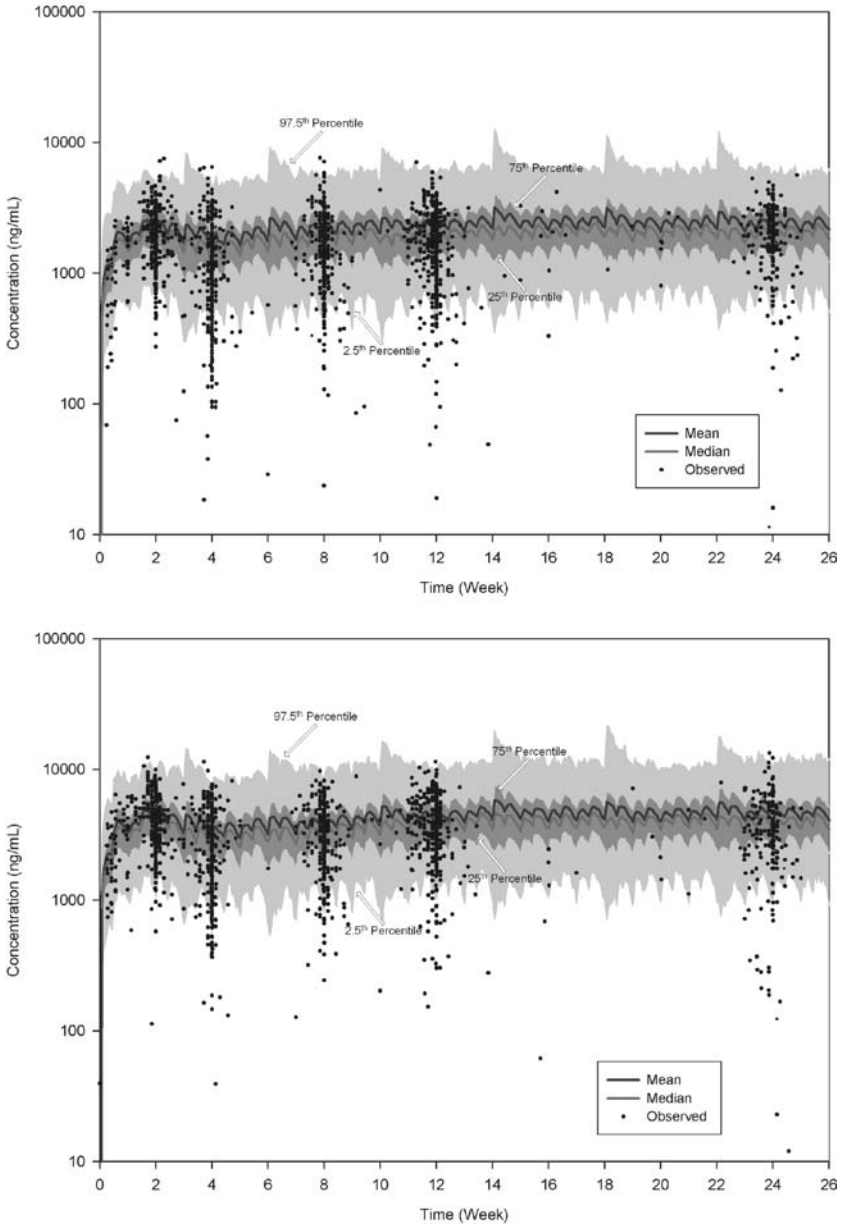

Fig. 4. Simulation of 25 mg BIW (upper panel) and 50 mg BIW (lower panel) dosing.

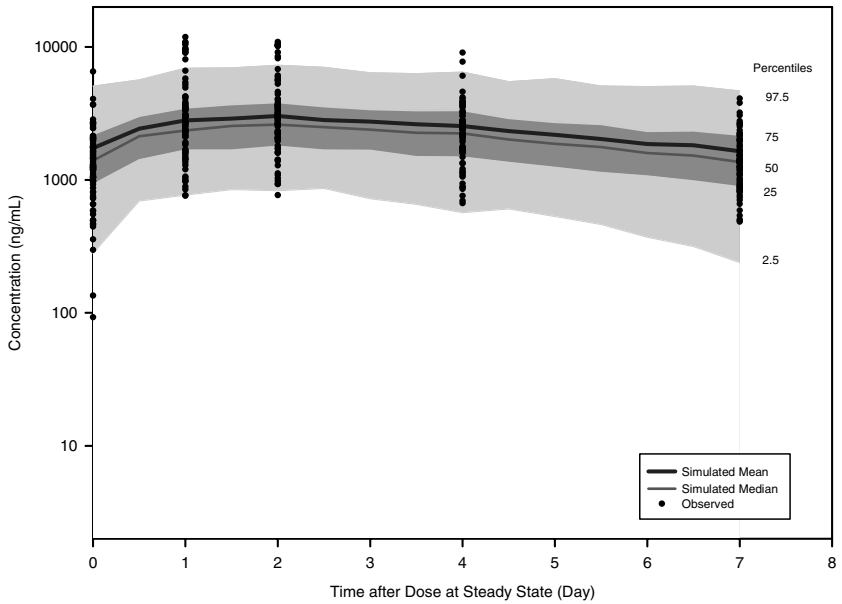

Fig. 5. Simulated 2.5, 25, 50, 75, and 97.5 percentiles during steady state of 50 mg once weekly dosing with the final population PK model (superimposed are the measured individual concentrations from Study 4 ($n = 84$)).

Figure 6 shows the simulated concentration–time profiles at steady state with the 25 mg BIW and 50 mg QW dosing regimens; the mean, 2.5th and 97.5th percentiles are presented. As expected there is a significant overlap between the two profiles indicating that the steady state exposures with both dosing regimens are very similar. The mean simulated maximum concentration with the 50 mg QW dosing regimen (3030 ng/ml, achieved at 48 h after the dose) is only about 16% higher than the mean simulated maximum concentration with the 25 mg BIW dosing regimen (2610 ng/ml, achieved at 24 h after the second dose of the BIW dosing). The mean simulated minimum concentration with the 50 mg QW dosing regimen (1640 ng/ml, achieved at the end of the dosing period) is about 20% lower than the mean simulated minimum concentration with the 25 mg BIW dosing regimen (2060 ng/ml, achieved at the end of the dosing period).

DISCUSSION

The final population PK model adequately describes the concentration–time profiles of etanercept in subjects with moderate to severe

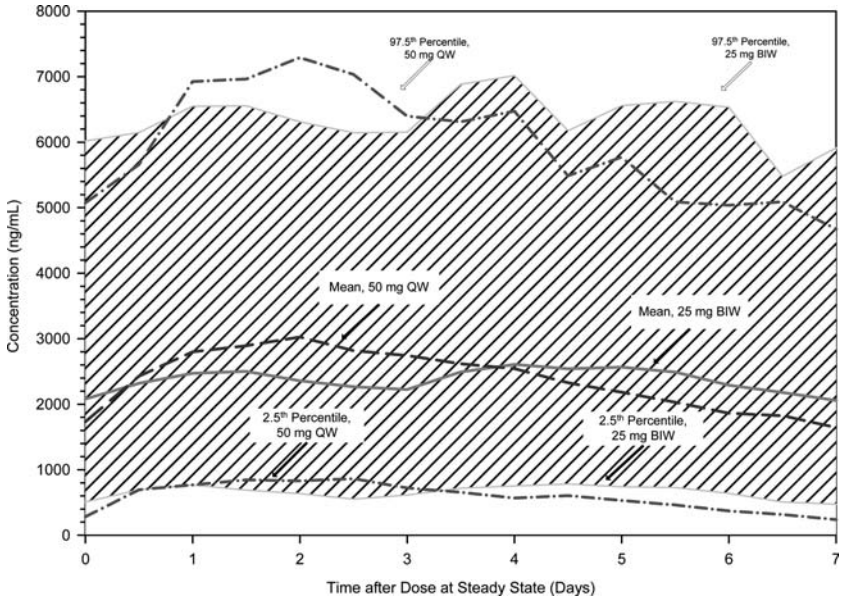

Fig. 6. Simulated concentration–time profiles at steady state with the 25 mg twice weekly and 50 mg once weekly dosing regimens. The mean, 2.5th, and 97.5th percentiles are presented (hatched areas denote the 2.5th and 97.5th percentiles of the 25 mg twice weekly dosing regimen).

plaque psoriasis. The basic structural population PK model has a relatively simple compartmental structure—one-compartment with linear absorption and elimination; attempts to fit a two-compartment model to the data failed. However, the current structure of the model is in line with the structure of the population PK model for SC administered etanercept in RA subjects (10). An alterative population PK model for etanercept in ankylosing spondylitis (14), developed recently, has a two-compartment structure, but this was made possible using data from both IV and SC administration. It can be assumed, therefore, that the ability to identify a second compartment for etanercept was a result of the presence of the IV data. With SC data only, the distribution phase in the concentration–time profiles is masked by the drug absorption process (with a half-life of approximately 24 h), which prevents the successful identification of a two-compartment model.

The limited amount of data from the true absorption phase in the current data set did not allow for the estimation of the IIV on the absorption constant K_a. All the IIV in pharmacokinetics seemed to be

accounted for by the variability assigned to the apparent clearance CL/*F* and volume of distribution *V*/*F*.

Unfortunately, no intravenous administration data were available in the psoriasis population (as well as in the RA population) so the important problem of identifying the real subcutaneous absorption profile of etanercept is still open. Mechanistically, the SC absorption process for an antibody-like construction should be a complex process, including at least two pathways, as a significant portion of the drug amount will reach the circulation through the lymph circulation. The potential of a flip-flop phenomenon here cannot be excluded, especially the lymph to blood transfer rate controlling the terminal portion of the curve. The PK sampling scheme limitations, however, would not permit further exploration of the issue in our case.

The apparent simplicity of the model structure is complicated by the necessity to introduce a relatively complex model of the existing variability. Similar to the RA case, the prolonged course of treatment for psoriasis as well as the underlying mechanisms of drug distribution and action required the introduction of IOV terms for the apparent clearance (CL/*F*) and apparent volume of distribution (V/*F*).

Despite a somewhat different covariate set, the parameter estimates of the population PK model for etanercept are very similar between the psoriasis and RA population, as indicated in Table V. A note of caution for the direct comparison of the parameters in the table is due—the typical clearance and volume values of the psoriasis patients are given for a 90 kg subject, while the typical clearance and volume values of the RA population are evaluated for a 70 kg RA patient (10). A conversion to the same body weight, using either the RA (10) or the psoriasis parameter models (Eqs. (4) and (5)), is necessary if those values are to be compared directly. The observed similarity shows that the serum pharmacokinetics of etanercept is not strongly influenced by the indication targeted.

The clearance values in Table V show that in psoriasis the gender differences are opposite, compared to RA—psoriatic males clear etanercept about 12% slower than females. The situation in RA is reversed—females have about 15% lower clearance than males. In both cases those differences seem to be significant, judging from the 95% confidence intervals estimated from boostraps. Fixing the clearance related exponent on the weight covariate may have contributed to the uncovering of this difference. Still, the gender differences in the clearances are too small, compared to the overall PK variability (in the region of 50% and more), to have any clinical significance. Similarly to the RA case, both the model parameter IIV and IOV are relatively high, corresponding to the high variability and uncertainty of the data. It can be noted

Table V. Comparison of the Population PK Model Parameters in Psoriasis and Rheumatoid Arthritis

		Psoriasis population PK model		RA population PK model (Lee et al., 2003)	
Parameter	Symbol	Covariates	Population mean[a] (95% CI¶)	Covariates	Population mean[b] (95% CI¶)
Clearance/F*	CL/F (l/h)	Male	0.129 (0.123~0.136)	Male, white	0.138 (0.118~0.163)
		Female	0.148 (0.137~0.161)	Female, white	0.117 (0.108~0.130)
		Time ≤ 180 h	0.733 (0.523~0.935)	Nonwhite (compared to white)	138.0% (104~160%)
		Time ≤ 360 h	0.780 (0.670~0.892)		
		Time ≤ 700 h	1.32 (1.24~1.41)		
		Time ≤ 1400 h	1.18 (1.11~1.26)		
		Time ≤ 2100 h	1.08 (1.03~1.13)		
		Time > 2100 h	1		
		Exponent on WTKG	0.668 (0.551~0.829)		0.75
Volume of distribution/F*	V/F (l)	Time ≤ 180 h	16.1 (10.1~20.7)		16.1 (14.3~18.2)
		Time ≤ 700 h	20.0 (12.8~24.8)		
		Time > 700 h	22.5 (13.9~30.7)		
		Exponent on WTKG	0.652 (0~0.973)		1
Absorption rate	K_a (hr^{-1})		0.0314 (0.0149~0.0533)		0.0332 (0.0246~0.0374)

*Calculated for a psoriasis subject weighing 90 kg (see text for detailed explanation), F = bioavailability; RA parameters are calculated for a RA subject weighing 70 kg, see (10).

¶Standard error of estimate, calculated from 929 bootstrap re-samplings.

[a]Based on a WTKG normalized to 90 kg.

[b]Based on a WTKG normalized to 70 kg.

that such high variability is not rare, especially for the PK of large protein molecules.

The results from the bootstrap procedure showed that the final model parameters were estimated with acceptable accuracy, given the high variability and uncertainty of the data. The clearance and related parameters were especially well characterized, while the precision of the volume of distribution and related parameters was somewhat lower, but still adequate.

The inability of the FOCE method (for a model without IOV) to improve the model, compared to the results of the FO method (for a model with IOV) indicates that the more refined estimation provided by the former method cannot compensate for the added flexibility provided by the inclusion of the IOV terms.

Of special interest is the identified time-dependence of the clearance and volume. Figure 7 shows the estimated time course of the apparent clearance (upper panel) and apparent volume of distribution (lower panel). After an initial sharp increase of at least 80%, the apparent clearance converges gradually to a new steady state level, which is approximately 30% higher than the week 1 value. From its week 1 value the apparent volume of distribution ascends monotonously to a steady state value, which is approximately 35% higher than the initial one. Such time dependence has been noted in one RA study (Study A in (10)) as well, where small, but statistically significant fluctuations in clearance and volume of distribution were observed.

The estimated time dependence of the PK parameters arises from the need to account for the observed fluctuation of the concentration–time profile between weeks 2 and 8. A similar fluctuation, but with much shorter duration, is observed in RA data (15). The latter suggests that a possible cause for the fluctuation is the complex cascade of both TNF and etanercept binding and redistribution processes between the blood compartment and the site of action compartment that commences after the administration of the drug. In psoriasis the site of action (skin) is a much larger and poorly perfused compartment, compared to the RA (synovium), which is much smaller and richly perfused. Consequently, the redistribution is more noticeable and takes longer to complete in psoriasis than in RA. It should be noted, however, that this hypothesis needs further mechanistic investigation.

Table IV indicates that some of the 95% confidence intervals of the time-dependent parameters related to clearance and volume overlap. It should be noted however, that in this case, the time dependent step function was used to provide a step-wise approximation of what are continuous processes of change in the clearance and volume. Therefore, it is probably more important to get a more detailed description of the

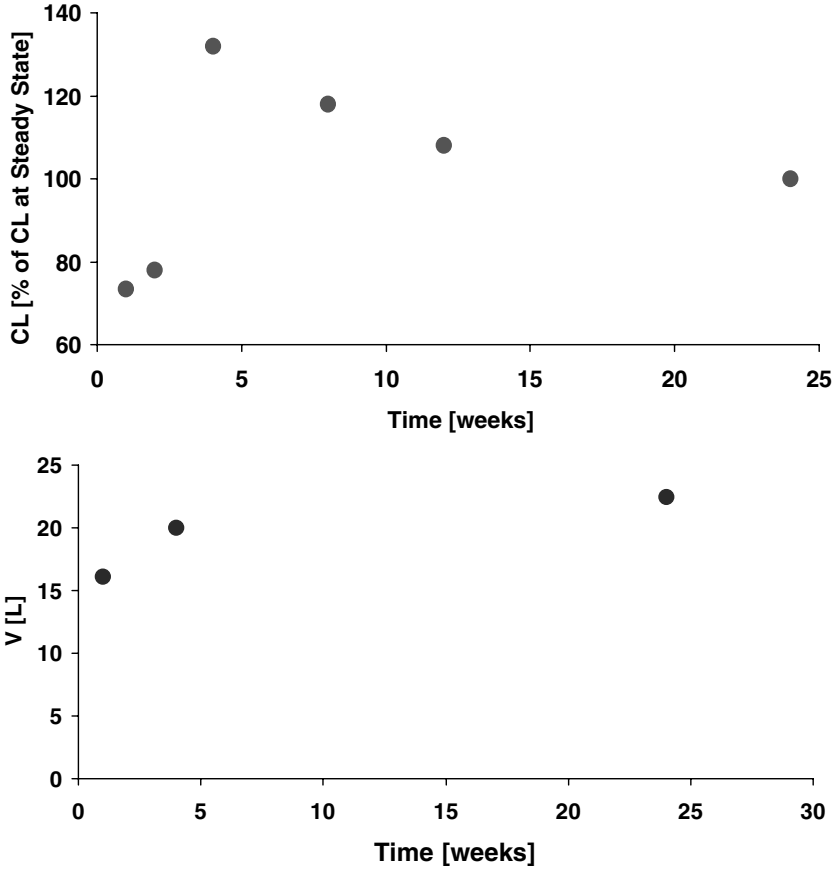

Fig. 7. Estimated time course of the apparent clearance (upper panel) and apparent volume of distribution (lower panel) from the final population PK model.

course of these continuous processes. What is more, the characteristic points of these relationships (e.g., minimum, maximum, steady state value) have confidence intervals that do not overlap. Any overlap between the 95% CI is conditioned upon the selection of the time thresholds (discretization intervals) and is should not be over-interpreted. Unfortunately, fitting a continuous function model the time fluctuations in clearance and volume lead to numerical problems and had to be abandoned as an alternative.

In both the clearance and the volume of distribution case, however, the effect of this fluctuation is a one off event, displayed at concentrations

well above those required for therapeutic benefit. Since this is a transient event and steady state is subsequently achieved, it is unlikely that these time dependencies have any clinical significance or implications.

The plot of the individual Bayesian predicted vs. the observed concentration values for the final model shows a slight bias towards over-prediction in the lower concentration range. Our numerical predictive experiments showed that part of this bias is due to the assumption of nominal dosing scheme for the majority of the patients as well to the presence of dosing irregularities (missed doses) that apparently were not properly recorded in the data set. Our analysis shows, however, that the major reason for the bias is the inadequate flexibility of the stepwise clearance and volume variation, adopted in the final population PK model, to accommodate the full swing of the concentration profile fluctuation. For this reason, the majority of the over-predicted values are located at the earlier time points—weeks 4 and 8. Unfortunately, our attempts to model a continuous change in the model parameters encountered serious numerical problems with NONMEM and were not successful.

The simulation exercise with the existing dosage regimens, which was carried out as part of the population PK model qualification, and the comparison of the predicted and observed concentration–time data, showed that the final model adequately describes both the central tendency and the variability of the data. The good agreement between the simulated profiles and the external data during the external model validation step serves as an additional qualification and indicates that the final population PK model can be used for extrapolation across dosing regimens in this case.

One of the objectives of the population PK model development was to explore by simulation the time course of the concentrations following a novel 50 mg QW dosing regimen and to compare them to the currently prescribed (for RA) 25 mg BIW dosage. Our simulations show that there is a significant overlap between the profiles indicating that the steady state exposures with both dosing regimens are very similar. Therefore their respective efficacy and safety profiles are likely to be similar as well.

ACKNOWLEDGMENTS

The clinical studies were conducted with the decisive participation of the members of the ENBREL® Psoriasis Study Group. Mrs. Ann Dugan assisted with the study conduct. Mr. Abosaleem Bassam coordinated the bioassay of the pharmacokinetic samples. Mrs. Mary Ann Simiens, Mrs. Nicole Coronado, Mrs. Claudia Sheelo, and Mr. Naren Narayanan

contributed to the technical preparation of this manuscript. This manuscript has been drafted during the employment of Dr. Ivan Nestorov with Amgen Inc.

REFERENCES

1. J. Koo. Population-based epidemiologic study of psoriasis with emphasis on quality of life assessment. *Dermatol. Clin.* **14**:485–496 (1996).
2. R. D. Granstein. New treatments for psoriasis. *N. Engl. J. Med.* **345**:284–287 (2001).
3. C. Bonifati and F. Ameglio. Cytokines in psoriasis. *Int. J. Dermatol.* **38**:241–251 (1999).
4. L. W. Moreland, M. H. Schiff, S. W. Baumgartner, E. A. Tindall, R. M. Fleischmann, K. J. Bulpitt, A. L. Weaver, E. C. Keystone, D. E. Furst, P. J. Mease, E. M. Ruderman, D. A. Horwitz, D. G. Arkfeld, L. Garrison, D. J. Burge, C. M. Blosch, M. L. M. Lange, N. D. McDonnell, and M. E. Weinblatt. Etanercept therapy in rheumatoid arthritis: A randomized, controlled trial. *Ann. Int. Med.* **130**:478–486 (1999).
5. M. E. Weinblatt, J. M. Kremer, A. D. Bankhurst, K. J. Bulpitt, R. M. Fleischmann, R. I. Fox, C. G. Jackson, M. Lange, and D. J. Burge. A trial of etanercept, a recombinant tumor necrosis factor receptor: Fc fusion protein, in patients with rheumatoid arthritis receiving methotrexate. *N. Engl. J. Med.* **340**:253–259 (1999).
6. P. J. Mease, B. S. Goffe, J. Metz, A. VanderStoep, B. Finck, and D. J. Burge. Etanercept in the treatment of psoriatic arthritis and psoriasis: A randomised trial. *Lancet* **356**:385–390 (2000).
7. C. L. Leondardi, J. L. Powers, R. T. Matheson, B. S. Goffe, R. Zitnik, A. Wang, and A. B. Gottlieb. Etanercept as a monotherapy in patients with psoriasis. *N. Engl. J. Med.* **349**:2014–2022 (2003).
8. J. M. Korth-Bradley, A. S. Rubin, R. K. Hanna, D. K. Simcoe, and M. E. Lebsack. The pharmacokinetics of etanercept in healthy volunteers. *Ann. Pharmacother.* **34**:161–164 (2000).
9. M. E. Lebsack, R. K. Hanna, M. A. Lange, A. Newman, W. Ji, and J. M. Korth-Bradley. Absolute bioavailability of TNF receptor fusion protein following subcutaneous injection in healthy volunteers (abstract). *Pharmacotherapy* **17**:1118–1119 (1997).
10. H. Lee, H. C. Kimko, M. Rogge, D. Wang, I. Nestorov, and C. C. Peck. Population pharmacokinetic (PK) and pharmacodynamic (PD) modeling of Etanercept using logistic regression analysis. *Clin. Pharmacol. Ther.* **73**:348–365 (2003).
11. I. Nestorov, R. Zitnik, C. Banfield, T. DeVries, and A. Wang. Pharmacokinetics of subcutaneously administered etanercept in patients with psoriasis. *J. Investig. Dermatol*, submitted for publication.
12. M. Karlsson and N. Jonsson. *Xpose 2.0 User's Manual*, Uppsala University, Uppsala, Sweden, 1998.
13. E. N. Jonsson and M. O. Karlsson. Xpose—an S-PLUS based population pharmacokinetic/pharmacodynamic model building aid for NONMEM. *Comp. Meth. Prog. Biomed.* **58**:51–64 (1999).
14. H. Zhou, M. Buckwalter, J. Boni, P. Mayer, D. Raible, J. Wajdula, S. Fatenejad, and M. Sanda. Pharmacokinetics (PK) of etanercept ankylosing spondylitis (AS) patients: a population-based investigation (abstract). *J. Clin. Pharmacol.* **43**:1033.
15. I. Nestorov, M. Lebsack, T. DeVries, and D. Burge. Pharmacokinetics of etanercept after once weekly subcutaneous administration of 50 mg doses to rheumatoid arthritis patients. Abstracts of the Annual European Congress of Rheumatology EULAR 2003. *Ann. Rheumat. Dis.* **62**(Suppl. 1):THU0239.
16. J. Parke, N. H. G. Holford, and B. G. Charles. A procedure for generating bootstrap samples for the validation of nonlinear mixed-effects population models. *Comp. Meth. Prog. Biomed.* **59**:19–29 (1999).